TWO-PHASE FLOWS WITHIN SYSTEMS WITH AMBIENT PRESSURE ABOVE THE THERMODYNAMIC CRITICAL PRESSURE

R.C. Hendricks
National Aeronautics and Space Administration
Lewis Research Center
Cleveland, Ohio 44135

M.J. Braun and R.L. Wheeler III
University of Akron
Akron, Ohio 44325

R.L. Mullen
Case Western Reserve University
Cleveland, Ohio 44106

In systems where the design inlet and outlet pressures P_{amb} are maintained above the thermodynamic critical pressure P_c, it is often assumed that two-phase flows within the system cannot occur. Designers rely on this simple rule of thumb to circumvent problems associated with a highly compressible two-phase flow occurring within the supercritical pressure system along with the uncertainties in rotordynamics, load capacity, heat transfer, fluid mechanics, and thermophysical property variations. The simple rule of thumb is adequate in many low-power designs but is inadequate for high-performance turbomachines and linear systems, where two-phase regions can exist even though P,amb > Pc. Rotordynamic-fluid-mechanic restoring forces depend on momentum differences, and those for a two-phase zone can differ significantly from those for a single-phase zone. Using the Reynolds equation the angular velocity, eccentricity, geometry, and ambient conditions are varied to determine the point of two-phase flow incipience. Subsequent dynamic effects and experimental verification remain as topics for future research.

SYMBOLS

a dimensionless eccentricity, e/C

C clearance, cm

D diameter, cm

e eccentricity

f,h functions scaling working fluid to reference fluid

G_r reduced mass flux, G/G*

G mass flux, g/s-cm^2

G^* thermodynamic parameter, $(P_c\rho_c/Z_c)^{1/2}$, 6010 g/s cm^2 for nitrogen

H fluid film thickness, cm

L spacer or bearing length, cm

ℓ aperture (orifice, Borda) length, cm

M molecular weight

N rotational speed, rad/sec (rpm)

P pressure, MPa

P_r reduced pressure, P/P_c

R radius, mm

R_g gas constant

S entropy, J/g K

T temperature, K

T_r reduced temperature, T/T_c

w mass flow rate, g/s

Z axial coordinate, cm

Z_0 compressibility factor, $P/\rho R_g T$

η viscosity, Pa-s

θ circumferential coordinate, rad

Λ bearing parameter

ρ density, g/cm^3

Φ,Θ shape functions

Ω angular velocity, rad/s

Subscripts:

amb ambient

c thermodynamic critical point (also superscript)

ex exit

in inlet

s saturation

0 reference fluid

α working fluid

INTRODUCTION

As a rule of thumb the extent and nature of the cavity formed downstream of the minimum clearance in a bearing or seal can be controlled, even eliminated, by increasing the ambient pressure. Even for systems operating above the thermodynamic critical pressure the rule of thumb - maintain the design inlet and outlet pressures well above the thermodynamic critical pressure - is used to circumvent two-phase flow and cavity formation (fig. 1). Uncertainties in stability, load capacity, heat transfer, fluid mechanics, and thermophysical property variations are thereby avoided. This simple rule of thumb usually works for low-power designs, but it is inadequate for high-performance turbomachines and linear systems.

In many cases the two-phase flow cavity enhances bearing stability (refs. 1 and 2) and seal load capacity (ref. 3). The inception of cavity flow is important to both turbomachine stability and load capacity.

Cavity flows are engendered by local "violations" of thermodynamics, termed "metastabilities." Classic among these are the fine capillary work of Skripov (ref. 4) and applied work such as fracture, boiling, and condensing (refs. 5 and 6).

Thus a two-phase flow cavity within a supercritical pressure system would be considered unstable, perhaps even unrealistic. Such conditions do not violate thermodynamics but are a source of incompatibility for the practicing engineer. Yet it has been demonstrated that two-phase cavity flows can be "nested" within a supercritical pressure system and that conditions for the existence of such nested cavities are prevalent for sharp-edge inlets and for eccentrically loaded high-performance turbomachines (ref. 7).

In this paper we will fix a turbomachine configuration, and for a series of parametric variations, establish a point of incipient two-phase flows by using the Reynolds equation and methods of corresponding states.

TURBOMACHINE CONFIGURATIONS

Normally seals and bearings for high-performance turbomachines operate at small eccentricities. However, during abnormal events or at high loads, the dimensionless eccentricity a can approach 1 (rubbing). The load W supported by a stable constant-property 360° fluid film H becomes (refs. 1 and 8)

C-2

$$\left(\frac{W}{A\ \Delta P}\right)_{theory} = \Lambda \frac{a}{(2 + a^2)\sqrt{1 - a^2}} \tag{1}$$

where Λ is the modified bearing parameter

$$\Lambda = \frac{6RL\eta\Omega}{C^2\ \Delta P} \tag{2}$$

and A the surface area, $A = 2\pi RL$. For a short bearing Holmes (ref. 1) gives

$$\left(\frac{W}{A\ \Delta P}\right)_{theory} = \frac{\Lambda}{48\pi}\left(\frac{L}{R}\right) \frac{a}{(1 - a^2)^2} \left[\pi^2 (1 - a^2) + 16a^2\right]^{1/2} \tag{3}$$

Departures from theory are represented by the normalized load capacity, which is obtained from integrating the numerically calculated pressure profiles

$$\text{Load capacity ratio} = (W/A\ \Delta P)_{calc}/(W/A\ \Delta P)_{theory} \tag{4}$$

Later we will make use of these relations in comparing full-film to incipient-film capacities.

Seals

Figure 2(a) illustrates the geometry of a high-performance turbomachine seal such as those used in the space shuttle main engine (SSME) (ref. 3). The working fluid is parahydrogen (P_c = 1.2928 MPa, T_c = 32.976 K, ρ_c = 0.0314 g/cm^3). The pressure profiles (fig. 2(b)) are for a fully eccentric, nonrotating shaft. The inlet pressure is greater than P_c, as is the pressure at the inlet to the third step. However, immediately downstream of the step the pressure on one "side" of the seal ($\theta = 0$) remains above P_c while the pressure on the opposite "side" ($\theta = \pi$) is nearly P_s. Thus the circumferential pressure profile possesses all states from $P_{in} > P_c$ at $\theta = 0$ to approximately $P_s < P_c$ at $\theta = \pi$, which represents two-phase cavity flow nested within a supercritical pressure regime.

With eccentric seals pressure gradients of sufficient magnitude can exist to engender two-phase cavity flows both axially and circumferentially while embedded or nested within a supercritical pressure system.

Bearings

Unlike those for a seal the axial pressure gradients for a bearing are usually small, but the circumferential gradients are usually much larger. Embedded two-phase cavity flow zones in seal flows have been established and should occur naturally in bearings. High-speed motion pictures (to 5000 pps) of the incipience, development, and collapse of the two-phase flow cavity and pressure-temperature profiles on the stator have been mapped for a low-performance machine (refs. 10 and 11). It is also noted in reference 10 that the two-phase zone begins to collapse as system ambient pressure is increased.

However, for calculations using Reynolds equations (ref. 11), a high-performance bearing configuration in fluid hydrogen at high eccentricity (table I) reveals a two-phase flow cavity embedded within the system where $P_{in} > P_{ex} > P_c$ (fig. 3). The cavity flow may be similar to that found for sharp-edge inlets (ref. 12). The pressure P drops abruptly from P_{in} to below P_s; in the recovery zone P increases to P_s; in the diffusion zone the pressure can recover or remain monotone; either case terminates in a two-phase choke (fig. 4).

The onset of the embedded two-phase flow cavity zone depends on the parameters of equation (1) and is prevalent at lower ambient pressure (e.g., one-tenth those of table I), high eccentricity, and high rotating speed and for large geometries. To illustrate the effects of two-phase flow cavity control, the pressure difference $(P_0 - P_{min})/P_c$ is tabulated (table II) as a function of running speed N for three eccentricities at two temperatures. A similar table (table III) was constructed for the load capacity ratio for numerically finite, infinitely short, and infinitely long bearings. The fluid is hydrogen. This effect remains to be verified experimentally. If it is correct, this demonstrates yet another method of achieving and controlling embedded two-phase flow cavities, which do not require a sharp geometrical configuration to "trigger" the event. Spontaneous nucleation within the metastable field is necessary and sufficient.

Using the principles of corresponding states, extensions to other single-component fluids (perhaps multicomponent fluids) appear reasonable (refs. 13 and 14) where viscosity becomes

$$\eta_\alpha (P,T) = \eta_0 \left(P \frac{h}{f}, \frac{T}{f} \right) F_\eta \tag{5}$$

and from equation (2)

$$\Lambda_\alpha (P,T) = \Lambda_0 \left(P \frac{h}{f}, \frac{T}{f} \right) F_\eta \tag{6}$$

where for single-component fluids

$$F_\eta = \frac{\left(\frac{M_\alpha}{M_0} f \right)^{1/2}}{h^{2/3}} \tag{7}$$

$$f = \left(\frac{T_\alpha^c}{T_0^c} \right) \Theta \tag{8}$$

$$h = \left(\frac{V_\alpha^c}{V_0^c} \right) \Phi = \frac{M_\alpha}{M_0} \frac{\rho_0^c}{\rho_\alpha^c} \Phi \tag{9}$$

for extensions to multicomponent fluids, which are complex (refs. 13 and 14). Example: Let the reference fluid (0) be oxygen and the working fluid (α) be nitrogen. The bearing temperature and pressure are 100 K and 1.5 MPa. Assuming constant properties and $\Theta = \Phi = 1$, solve equation (2) for nitrogen by using the thermophysical properties of oxygen. First we need the thermodynamic properties at the critical point.

Fluid	T_c, K	P_c, MPa	ρ_c, g/cm^3	M, g/g-mole	Θ	Φ	f	h	F_η
N_2	126.3	3.417	0.3105	28.016	1	1	0.816	1.22	0.74
O_2	154.78	5.082	.4325	31.9988					

$$f = 126.3/154.78 \times 1 = 0.816 \; ; \; h = (28.016/31.9988)(0.4325/0.3105) \times 1 = 1.22$$

$$F_\eta = [(31.9988/28.016)\ 0.816]^{0.5}/1.22^{(2/3)} = 0.74$$

$$P_0 = P(f/h) = 1.5\ (1.22/0.816) = 2.242 \text{ MPa}$$

$$T_0 = T/f = 100/0.816 = 122.5 \text{ K.}$$

From the thermophysical properties of oxygen (e.g., ref. 15) the viscosity at (P_0,T_0) is 0.936×10^{-3} g/cm s. The predicted nitrogen viscosity then becomes

$$\eta_0 F_\eta = 0.936 \times 10^{-3} \times 0.74 = 0.693 \times 10^{-3} \text{ g/cm s}$$

From the thermophysical properties of nitrogen (ref. 15) the viscosity at (P,T) is 0.777×10^{-3} g/cm s, which represents a 12-percent error. Once the bearing geometry and speed are defined, the solution to equation (2) follows from equation (5)

$$\frac{\Lambda\ (P,T)}{\Lambda\ (P_0,T_0)} = 0.74$$

to within 12 percent.* Reynolds equation (ref. 11) is now solved once using the bearing parameter for nitrogen at $P = 1.5$ MPa and $T = 100$ K and again using the bearing parameter predicted for nitrogen from oxygen properties at $P_0 = 2.242$ MPa and $T = 122.5$ K. The reduced circumferential pressure profiles at the center of the bearing, with speed as a parameter, are illustrated in figure 5.

Boilers and Rotors

A corollary class of nested two-phase flows occurs in turbomachine systems as rotating boilers and cooled rotor windings and in a multiplicity of superconducting machinery applications.

---

*In reference 11 the solution of the Reynolds equation is in dimensional form and $\Delta P \equiv 1$ (pressure units). For solutions that are in dimensionless form, with fixed P_{amb} and both P_0 and P much larger than P_{amb}, then $\Lambda/\Lambda_0 = fF_\eta/h$.

A pressure containment vessel, axial flow of a cooling (heating) fluid, and rotation of the fluid about an axis parallel to the flow path result in centrifugal and Coriolis body forces, which in turn produce pressure and shear forces within the fluid. Further, the radial position of the critical pressure surface can be adjusted to occur very close to the fluid-vapor interface.

For a cylindrical boiler rotating at N-rpm the fluid to be evaporated is forced against the outer wall at a pressure $P_{wall} = P_c$; for all $M > N$ P_{wall} is greater than P_c and vapor moves from the wall to the region where $P < P_c$; the two-phase region is nested. Here the Coriolis forces are small, but cannot be neglected when, for example, cooling a superconducting motor (generator) to prevent the winding from going normal. Again the pressure in the winding coolant tube becomes greater than P_c for all $M > N$ while the pressure at the centerline of rotation is less than P_c; the system is weakly nested. In this case two-phase flow can occur within the coolant tube and become distributed in an unusual axial pattern because of the Coriolis forces. In some instances it may be possible to find a spiral weakly nested region.

To the dynamicist the location and extent of the nested regions may become important only after the system instabilities are encountered.

SUMMARY OF RESULTS

Two-phase cavity flow zones have been shown to be embedded within a supercritical pressure envelope. For a fixed geometrical configuration these zones are established by controlling inlet stagnation conditions, exit backpressure, or combinations. The zones can be "triggered" by discontinuous changes in geometry or by significant pressure gradients.

For high-performance turbomachine seals and possibly bearings, nested two-phase zones can be found in the circumferential and axial coordinates. By using the Reynolds equation a surface of incipient two-phase flows was established. The load capacity of the bearing degrades significantly but not before an overshoot occurs. It is speculated that this overshoot "saves" the design. With the corresponding-states relations these results can be extended to other fluids. These phenomena remain to be demonstrated experimentally.

REFERENCES

1. Holmes, R.: On the Role of Oil-Film Bearings in Promoting Shaft Instability: Some Experimental Observations. NASA CP-2133, 1980, pp. 345-357.

2. Bently, D.E.; and Muszynska, A. : Stability Evaluation of Rotor/Bearing System by Perturbation Tests. NASA CP-2250, 1982, pp. 307-322.

3. Hendricks, R.C.: A Comparative Evaluation of Three Shaft Seals Proposed for High Performance Turbomachinery. Presented at the ASLE/ASME Joint Lubrication Conference, Washington, DC, Oct. 5-7, 1982. NASA TM-83021, 1982.

4. Skripov, V.P.: Metastable Liquids. John Wiley, New York, 1974.

5. Frenkel, J.: Kinetic Theory of Liquids. Dover Publications, New York, 1955.

6. Hendricks, R.C.; Mullen, R.L.; and Braun, M.J.: Analogy Between Cavitation and Fracture Mechanics. ASME/JSME Thermal Engineering Conference, March 21-26, 1983, Honolulu, Hawaii.

7. Hendricks, R.C.; Braun, M.J.; Wheeler, R.L.; and Mullen, R.L.: Nested Supcritical Flows Within Supercritical Systems. 20th Annual Cavitation and Multiphase Flow Forum, Albuquerque NM, June 24-26, 1985.

8. Crandall, S.H.: Heuristic Explanation of Journal Bearing Instability. NASA CP-2250, 1982, pp. 274-283.

9. Childs, D.W.; Hendricks, R.C.; and Vance, J.M., eds.: Rotordynamic Instability Problems in High-Performance Turbomachinery. Proceedings of a Workshop held at Texas A&M University, May 12-14, 1980. NASA CP-2133. (See also NASA CP-2250 (1982) and NASA CP-2338 (1984)).

10. Braun, M.J.; and Hendricks, R.C.: An Experimental Investigation of Vaporous/Gaseous Cavity Characteristics of an Eccentric Shaft Seal (or Bearing). Presented at the ASLE/ASME Joint Lubrication Conf. Washington, DC, Oct 5-7, 1982. ASLE Trans. vol. 27, no. 1, pp. 1-14, 1982.

11. Braun, M.J.; and Hendricks, R.C.: An Experimental Investigation of the Effect of Pressure and Temperature Levels on the Development and Nature of the Cavitation Region in a Submerged Journal Bearing. Bioengineering and Fluids Engineering Conference, Univ. of Houston, Houston, TX, June 20-22, 1983, ASME Bound Volume G00223.

12. Hendricks, R.C.; and Stetz, T.T.: Flow Through Aligned Sequential Orifice-Type Inlets. NASA TP-1967, 1982.

13. Mollerup, Jorgen: Correlated and Predicted Thermodynamic Properties of LNG and Related Mixtures in the Normal and Critical Regimes. Advances in Cryogenic Engineering, K.D. Timmerhaus (ed.), vol. 20, Plenum Press, New York, pp. 172-194.

14. Hendricks, R.C.; and Sengers, J.V.: Application of the Principle of Similarity to Fluid Mechanics. Water and Steam: Their Properties and Current Industrial Applications. 9th International Conference on Properties of Steam, J. Straub and K. Scheffler, eds., Pergamon Press, Oxford, 1980. Unabridged version as NASA TM X-79258, 1979.

15. Hendricks, R.C.; Baron, A.K.; and Peller, I.C.: GASP - A Computer Code for Calculating the Thermodynamic and Transport Properties for Ten Fluids: Parahydrogen, Helium, Neon, Methane, Nitrogen, Carbon Monoxide, Oxygen, Fluorine, Argon, and Carbon Dioxide. NASA TN D-7808, 1975.

TABLE I. - BEARING PARAMETERS FOR ANALYTICAL SOLUTION

Geometry:	
Diameter, mm (in)	25.4 (1)
Length, mm (in)	25.4 (1)
Clearance, mm (in)	0.0254 (0.001)
Eccentricity	0.97
Hydrodynamic:	
Inlet pressure, MPa (psia)	13.8 (2000)
Outlet pressure, MPa (psia)	13.45 (1950)
Maximum pressure, MPa (psia)	27.16 (3938)
Minimum pressure, MPa (psia)	0.079 (11.5)
Inlet temperature, K (°R)	20 (36)
Rotational speed, rad/s (rpm)	7850 (75 000)

TABLE II. - CAVITY PRESSURE DIFFERENCE $(P_{in} - P_{min})/P_c$ ALONG CENTERLINE

[Clearance, 0.076 mm (0.003 in); radius, 38 mm (1.5 in); spacer or bearing length, 76 cm (3 in); inlet pressure, 1.628 MPa (236 psia); exit pressure, 1.524 MPa (221 psia); viscosity, 0.127×10^{-4} Pa-s (0.187×10^{-8} lbf-s).]

Inlet temperature, T_{in}		Dimensionless eccentricity, a	Rotational speed, N, rpm		
K	°R		10×10^3	50×10^3	100×10^3
22.1	39.8	0.1	0.041	0.043	0.046
		.5	.045	.064	.087
		.95	.24	.646	-----
28.1	50.5	0.1	0.041	0.042	0.044
		.5	.043	.056	.071
		.95	.18	-----	-----

TABLE III. - LOAD CAPACITIES FOR NUMERICALLY FINITE, INFINITELY SHORT, AND INFINITELY LONG BEARINGS

[Clearance, 0.076 cm (0.003 in); radius, 38 mm (1.5) in); length, 76 cm (3 in); inlet pressure, 1.628 MPa (236 psia); exit pressure, 1.524 MPa (221 psia); viscosity, 0.127×10^{-4} Pa-s (0.187×10^{-8} lbf-s).]

Inlet temperature, T_{in}		Dimensionless eccentricity, a	Rotational speed, N, rpm	Bearing parameter, Λ	Numerically finite bearing	Infinitely short bearing	Infinitely long bearing	Pinkus/ Sternlicht
K	°R							
22.1	39.8	0.1	10×10^3	5.87	0.99	0.71	4.1	1.4
			50	29.3	4.9	3.5	20.6	7.2
			100	58.7	9.9	7.1	41.3	14.3
		.5	10	5.87	6.3	6.6	21.2	2.6
			50	29.3	31.3	33.1	106	13.2
			100	58.7	62.7	66.1	212	26.4
		.95	10	5.87	53	863	87	20
			50	29.3	265	4318	433	100
			100	58.7	-----	-----	-----	200
28.1	50.5	0.1	10×10^3	3.9	0.66	0.47	2.7	-----
			50	19.5	3.3	2.3	13.7	-----
			100	39.1	6.6	4.7	27.5	-----
		.5	10	3.9	4.2	4.4	14.1	-----
			50	19.5	20.9	22	70.6	-----
			100	39.1	41.7	44	141	-----
		.95	10	3.9	35.4	574	57.7	-----

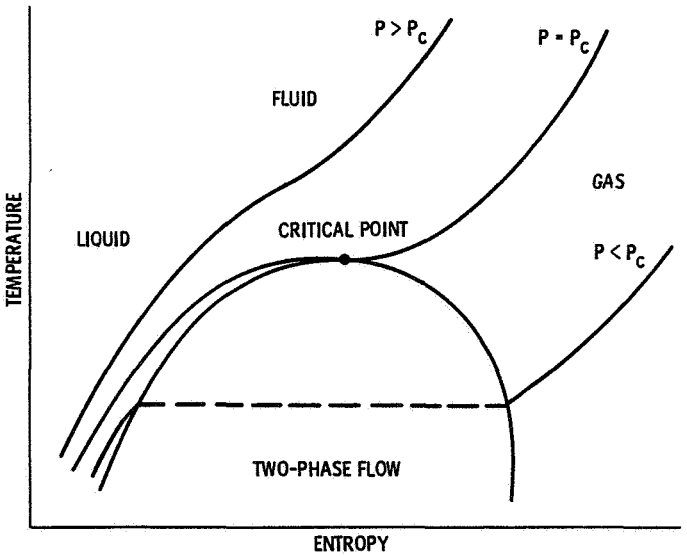

Figure 1. - Temperature-entropy schematic.

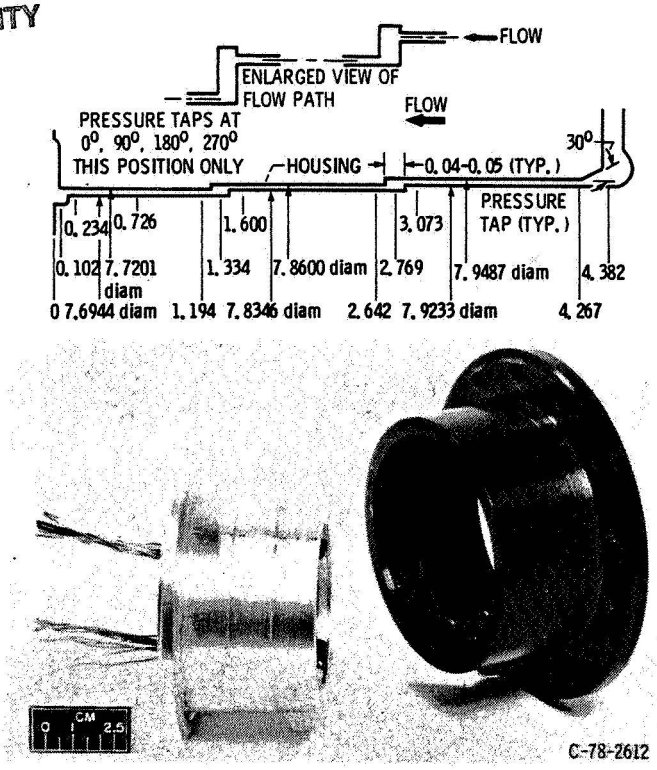

(a) Three-step shaft seal.

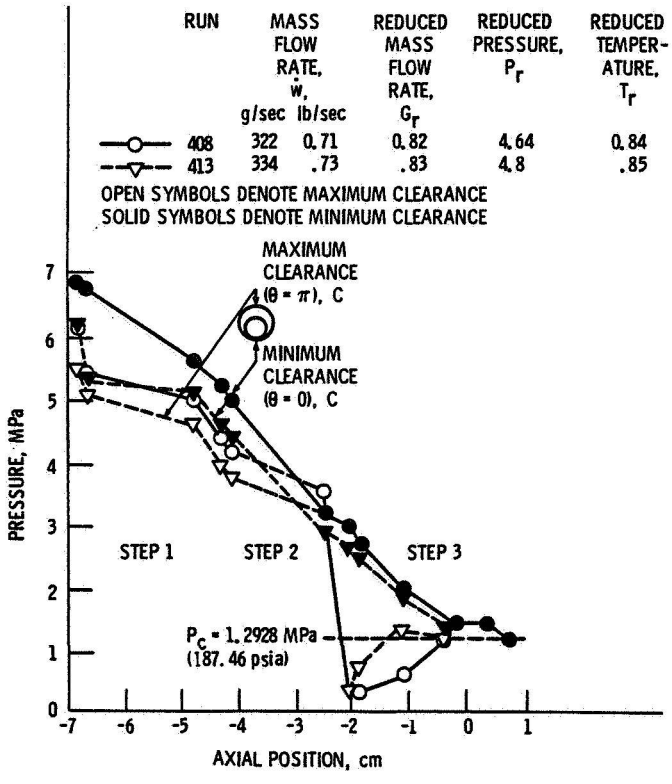

(b) Applied backpressure.

Figure 2. - Pressure profile for fully eccentric, nonrotating, three-step SSME seal configuration.

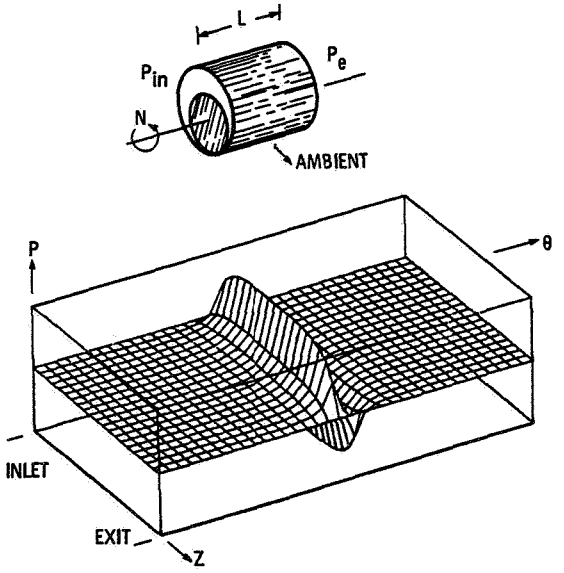

Figure 3. - Analytical pressure map for high-speed journal bearing with $P_{in} > P_e > P_c$; P_{in} = 13.8 MPa (2000 psi); P_e = 13.45 MPa (1950 psi); N = 75 000 rpm; $e_x = e_y = 0.68$; T_{in} = 20 K (36 ^{0}R); P_{amb} = 0.1 MPa (14.7 psi); T_{amb} = 56 K (100 ^{0}R).

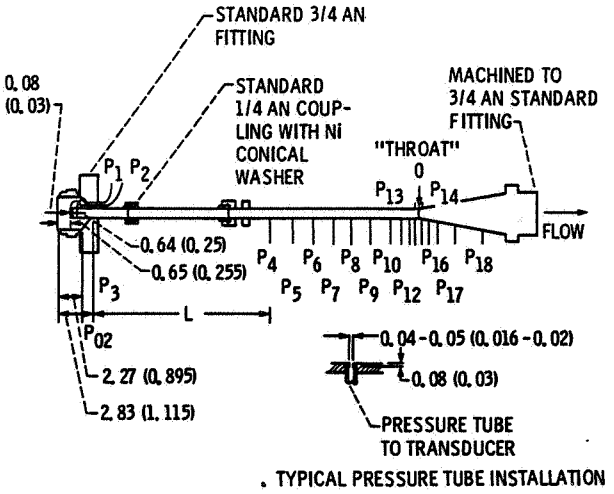

(a) Configuration geometry.

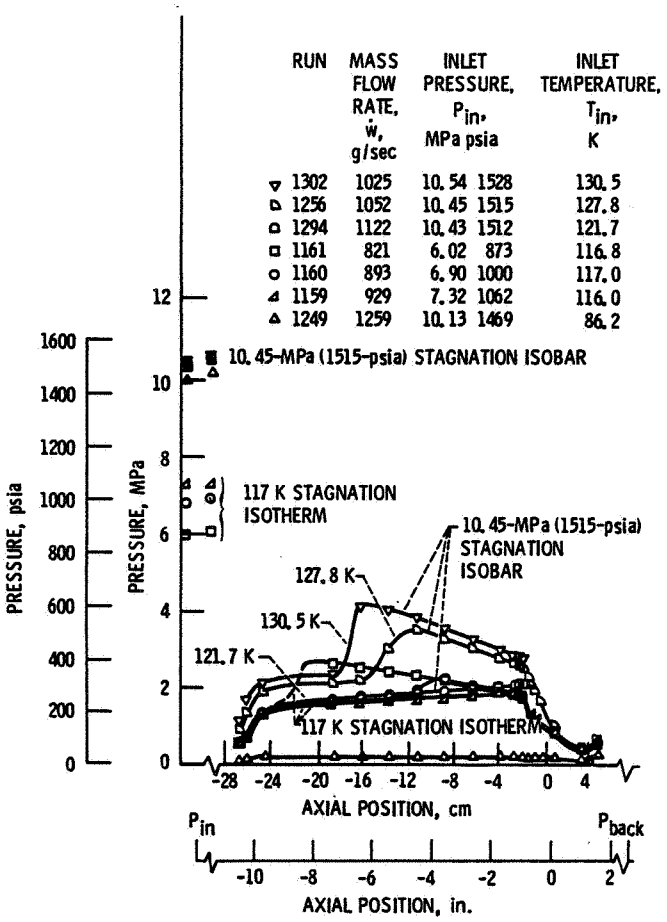

(b) Controlled inlet stagnation conditions.

Figure 4. - Pressure profile for nitrogen flow through high-L/D tube with Borda inlet. (Dimensions are in centimeters (inches).)

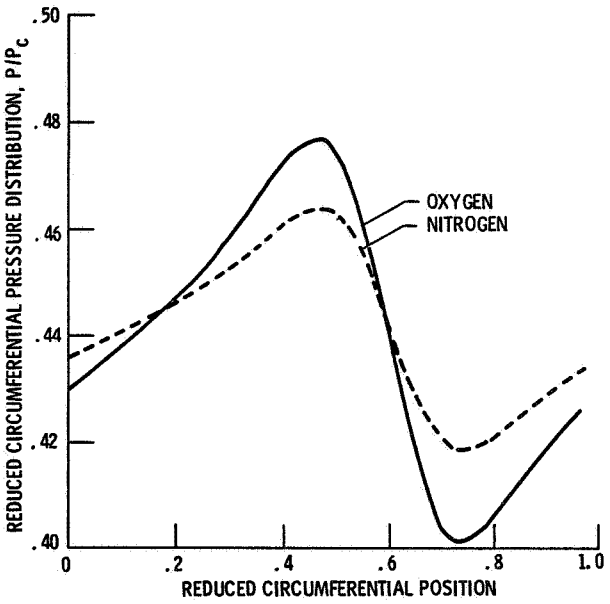

Figure 5. - Reduced midbearing circumferential pressure profiles based on corresponding states for fluids nitrogen and oxygen.